Since January 2020 Elsevier has created a COVID-19 resource centre with free information in English and Mandarin on the novel coronavirus COVID-19. The COVID-19 resource centre is hosted on Elsevier Connect, the company's public news and information website.

Genomics 113 (2021) 3449–3460

Contents lists available at ScienceDirect

Genomics

journal homepage: www.elsevier.com/locate/ygeno

Co-expression of the SARS-CoV-2 entry molecules ACE2 and TMPRSS2 in human ovaries: Identification of cell types and trends with age

Meng Wu [1], Lingwei Ma [1,1], Liru Xue, Qingqing Zhu, Su Zhou, Jun Dai, Wei Yan, Jinjin Zhang [*], Shixuan Wang [*]

Department of Obstetrics and Gynecology, Tongji Hospital, Tongji Medical College, Huazhong University of Science and Technology, Wuhan, Hubei, China

ARTICLE INFO

Keywords:
SARS-CoV-2
ACE2
TMPRSS2
Single-cell RNA-Seq
Ovary

ABSTRACT

The high rate of SARS-CoV-2 infection poses a serious threat to public health. Previous studies have suggested that SARS-CoV-2 can infect human ovary, the core organ of the female reproductive system. However, it remains unclear which type of ovarian cells are easily infected by SARS-CoV-2 and whether ovarian infectivity differs from puberty to menopause. In this study, public datasets containing bulk and single-cell RNA-Seq data derived from ovarian tissues were analyzed to demonstrate the mRNA expression and protein distribution of the two key entry receptors for SARS-CoV-2—angiotensin-converting enzyme 2 (ACE2) and type II transmembrane serine protease (TMPRSS2). Furthermore, an immunohistochemical study of ACE2 and TMPRSS2 in human ovaries of different ages was conducted. Differentially expressed gene (DEG) analysis of ovaries of different ages and with varying ovarian reserves was conducted to explore the potential functions of ACE2 and TMPRSS2 in the ovary. The analysis of the public datasets indicated that the co-expression of ACE2 and TMPRSS2 was observed mostly in oocytes and partially in granulosa cells. However, no marked difference was observed in *ACE2* or *TMPRSS2* expression between young and old ovaries and ovaries with low and high reserves. Correspondingly, ACE2 and TMPRSS2 were detected in the human ovarian cortex and medulla, especially in oocytes of different stages, with no observed variations in their expression level in ovaries of different ages, which was consistent with the results of bioinformatic analyses. Remarkably, DEG analysis showed that a series of viral infection-related pathways were more enriched in ACE2-positive ovarian cells than in ACE2-negative ovarian cells, suggesting that SARS-CoV-2 may potentially target specific ovarian cells and affect ovarian function. However, further fundamental and clinical research is still needed to monitor the process of SARS-CoV-2 entry into ovarian cells and the long-term effects of SARS-CoV-2 infection on the ovarian function in recovered females.

1. Introduction

The coronavirus disease 2019 (COVID-19) caused by SARS-CoV-2 (previously known as 2019-nCoV) imposes a major threat to the world's public healthcare systems. The critically ill patients can rapidly progress to clinical complications, including acute respiratory distress syndrome (ARDS), septic shock, coagulation dysfunction and even multiple organ failure. Elderly patients and those with underlying health conditions are prone to have a relatively high mortality. Person-to-person transmission of COVID-19 has been repeatedly reported in both in-hospital and household clustering [1].

According to Zhou et al. [2], SARS-CoV-2 is a novel coronavirus belonging to the subgenus *Sarbecovirus* within the genus *Betacoronavirus* (lineage B) and shares 79.5% of the genetic sequence with SARS-CoV. The SARS-CoV-2 genome encodes four structural proteins; the most important of these—the spike (S) protein utilizes angiotensin-converting enzyme 2 (ACE2) as a cell receptor to facilitate the virus entry into the host cell and cell membrane fusion [3,4]. Recent studies suggest that the cellular entry of SARS-CoV-2 also depends on type II transmembrane serine protease (TMPRSS2) [5,6]. TMPRSS2 primes the viral spike protein, allowing for the potent binding of ACE2, and induces virus-cell fusion. The above findings indicate that the exploration of *ACE2* and *TMPRSS2* expression in human tissues can predict the potentially infected cells and their respective effects in COVID-19 patients.

A series of bioinformatic analyses and experimental verifications have revealed that *ACE2* and *TMPRSS2* are expressed in the

* Corresponding authors.
E-mail addresses: jinjinzhang@tjh.tjmu.edu.cn (J. Zhang), sxwang@tjh.tjmu.edu.cn (S. Wang).
[1] The authors consider that the first two authors should be regarded as joint First Authors.

https://doi.org/10.1016/j.ygeno.2021.08.012
Received 16 September 2020; Received in revised form 2 August 2021; Accepted 14 August 2021
Available online 18 August 2021

Table 1
The sources of RNA-seq data from ovarian tissues used in this study.

GEO accession number	Species	Tissue or specific cells	Sample Number	Data Type	Cell number	Reference
GSE130664 (scRNA-seq)	*Macaca fascicularis*	Ovarian single cells	8	Raw counts matrix	2601	[20]
GSE107746 (scRNA-seq)	*Homo sapiens*	Oocytes and granulosa cells	7	Normalized expression matrix	151	[21]
GSE81579 (bulk RNA-seq)	*Homo sapiens*	Cumulus cells	20	Raw counts matrix	*	[42]
GSE87201 (bulk RNA-seq)	*Homo sapiens*	Oocytes	35	Normalized expression matrix	*	[43]
GTEx portal (bulk RNA-seq)	*Homo sapines*	Ovarian tissue	178	Normalized expression matrix	*	[18]

* Standard RNA-seq.

gastrointestinal tract, heart, lungs, and kidneys, demonstrating tissue-specific activity patterns [7–10]. In addition to causing lung damage such as ARDS, SARS-CoV-2 has been found to cause kidney, liver, and heart damage and gastrointestinal symptoms [11]. Most recently, Bian et al. [12] reported that SARS-CoV-2 RNA and viral particles were detected in multiple organs and tissues including the testis and ovary, which indicated that SARS-Cov-2 can reach the reproductive organs. Pathological analysis of the testes displayed varying degrees of spermatogenic cell reduction and damage. Using public datasets, Wang and colleagues [13] also provided evidence that the human testis are a potential target site of SARS-CoV-2 infection. The ovary is the core of the female reproductive system, and damage to it can cause infertility and premature ovary failure. One recent study did not detect significant expression of either ACE2 or TMPRSS2 in normal human ovaries by exploring a single-cell sequencing dataset [14], while another study reported that some oocytes in nonhuman primate ovarian tissue were found to express ACE2 and TMPRSS2 by analyzing transcriptomic and proteomic data [15]. However, such analyses have limitations; no verified experiments were conducted and they cannot be considered conclusive. Moreover, a detailed analysis of ACE2 and TMPRSS2 in the ovary from puberty to menopause was lacking; such an analysis is critically important to explore whether the ovaries of women of different ages will be affected by SARS-CoV-2.

In the present study, we investigated the *ACE2* and *TMPRSS2* mRNA expression profiles in the human ovary at bulk and single-cell resolution. We also analyzed the co-expression of *ACE2* and *TMPRSS2* in human ovary sections of women of different ages. Our study revealed that approximately 80% of the ovarian cells were positive for *ACE2* and *TMPRSS2*; they are predominantly enriched in oocytes and matrix cells of human ovaries. Additionally, there was no observed variation in *ACE2* and *TMPRSS2* expression in ovaries of different ages, consistent with the results of RNA sequencing analysis. In addition, we explored the expression of another receptor, basigin (BSG/CD147), and the cathepsins L (CTSL), which have residual cleavage activity toward the viral S protein [4] [16]; the results indicated that BSG and CTSL are expressed in somatic ovary cells. Our findings reveal that the receptors for SARS-CoV-2 are expressed in human ovaries and suggests that SARS-CoV-2 may potentially infect ovary.

2. Materials and methods

2.1. Ethical approval and human sample collection

The experiments conducted in the study were ratified by the Human Research Ethics Committee of Tongji Hospital, Tongji Medical College, Huazhong University of Science and Technology. All patients provided written informed consent. Ovarian tissues were obtained from six women at Tongji Hospital for the following indications: adenomyosis, cervical adenocarcinoma cancer, endometrial cancer, and benign ovarian mass. No pathological abnormality was observed in the ovarian samples by the pathologist.

2.2. Bulk RNA-Seq data collection and processing

The bulk RNA-Seq data from the Genotype-Tissue Expression (GTEx) database from 7845 samples of diverse normal human tissues were downloaded from UCSC Xena (https://xenabrowser.net/datapages/). As GTEx provides the complete data regarding sample collection, RNA-Seq experiments, quality control, and gene expression normalization, such information is not reproduced here [17,18]. The downloaded data were analyzed using "ggstatsplot" package in R to visualize the expression level of *ACE2* in multiple tissues. The Kruskal-Wallis test was used to analyze the difference of expression level between the lung and other organs. To identify the differentially expressed genes (DEGs) from old and young ovaries, we retrieved 178 ovarian samples (Table S1) collected from of different age stages (20–29 yr, 22 samples; 30–39 yr, 14 samples; 40–49 yr, 36 samples; 50–59 yr, 61 samples; and 60–79 yr, 45 samples) from GTEx and divided the samples into old (>40 yr) and young (<40 yr) groups; further analysis was performed using the DESeq2 package. Moreover, the DEGs in dataset GSE81579 were also analyzed using the "limma" package. DEGs were identified using the criteria $|\log_2(\text{fold change})| > 1$ and adjusted P_value <0.05. The results of the DEG analysis were displayed as volcano plots, with visualization of the genes *ACE2* and *TMPRSS2*.

2.3. Single-cell RNA sequencing data collection and processing

Two single-cell RNA sequencing (scRNA-Seq) datasets GSE130664 and GSE107746 were downloaded from the Gene Expression Omnibus (GEO) database (https://www.ncbi.nlm.nih.gov/geo/) with accession numbers GSE130664 (species: *Macaca fascicularis*) and GSE107746 (species: *Homo sapiens*) (Table 1). The scRNA-Seq dataset analysis followed the process described below. The unique molecular identifier (UMI) counts per gene per cell were processed using the "Seurat" package in R (version 3.1.4) [19]. After creating the Seurat object, further quality control was conducted. Cells were discarded if <50 genes were expressed and > 5% of reads were mapped to the mitochondrial genome. Genes expressed in fewer than three cells were also removed. Then, the gene expression data were normalized by log transformation using the "NormalizeData" function (selection.method = "LogNormalize"). After extracting 2000 highly variable genes (HVGs) with the "FindVariableGenes" function, the data matrix was centered and scaled using the "ScaleData" function. For cell clustering and linear dimensional reduction, we performed principle component analysis (PCA) on the HVGs using the "RunPCA" function. To reduce the technical noise, the "JackStraw" procedure was used to determine the PCA dimensionality of the analysis through permutation calculation. Twenty principal components were selected using the "ScoreJackStraw" function for further analysis. The next step was performed using the "FindNeighbors" and "FindClusters" functions; cells were clustered based on a graph-based clustering approach with the resolution as 0.5. A non-linear dimensionality reduction technique was implemented by running the "RunTSNE" and "TSNEPlot" functions. T-distributed stochastic neighbor embedding (t-SNE) plots were thus produced by projecting these datasets onto a two-dimensional space. To find cluster biomarkers, the "FindMarkers" function was used, and the curated known cell markers according to the available publications [20,21] and CellMarker database [22] were utilized to annotate the cell clusters. Then, the *ACE2/TMPRSS2* expression of distinct cell types was evaluated and visualized. To further analyze the DEGs between *ACE2/TMPRSS2*-positive and

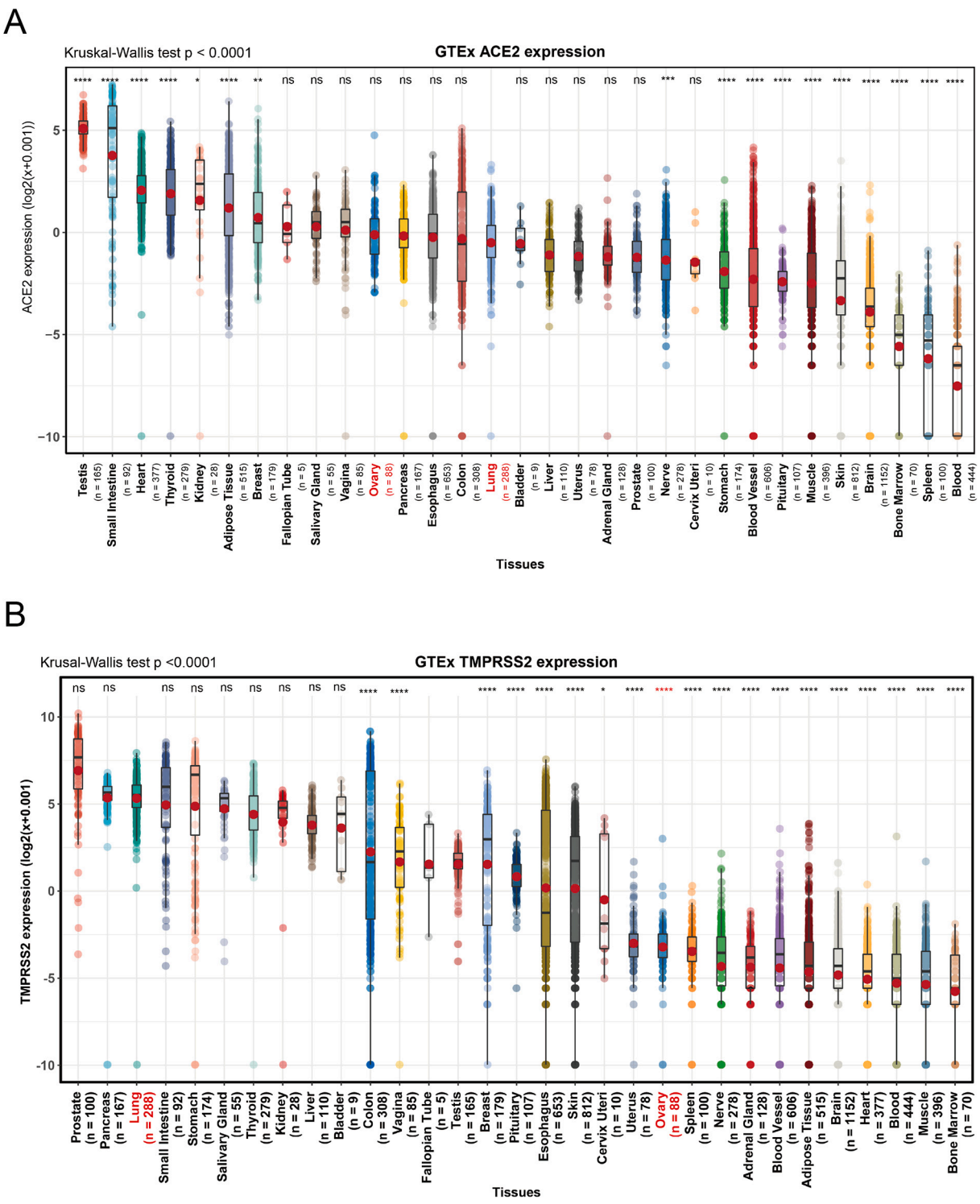

Fig. 1. mRNA expression levels of *ACE2* (A) and *TMPRSS2* (B) in multiple organs; data obtained from the Genotype-Tissue Expression (GTEx) database (a human organ database); * $p < 0.05$, ** $p < 0.001$, *** $p = 0.0001$, **** $p < 0.0001$. The vertical coordinates represent the log transformed (log2 [x + 0.001]) relative expression level of *ACE2* and *TMPRSS2*.

ACE2/TMPRSS2-negative cells, the function "FindMarkers" was used to generate a list of DEGs. Gene ontology (GO) and Kyoto Encyclopedia of Genes and Genomes (KEGG) functional enrichment pathway analysis were conducted using clusterProfiler [23].

2.4. Immunohistochemistry

The expression pattern of ACE2 and TMPRSS2 in human ovarian tissues was analyzed by immunohistochemistry. Ovarian tissues from human were formalin-fixed and paraffin-embedded. The 5-μm-thickness serial sections were processed by routine procedures. The sections were deparaffinized and rehydrated through gradient series of ethanol (100%, 95%, 85%, 75%). Then the slides were incubated in 3% H_2O_2 for inactivation of endogenous peroxidase and were microwaved for 15 min in citrate buffer (pH = 6.0) for antigen retrieval. After cooling at room temperature, slides were blocked with 5% BSA without washing in

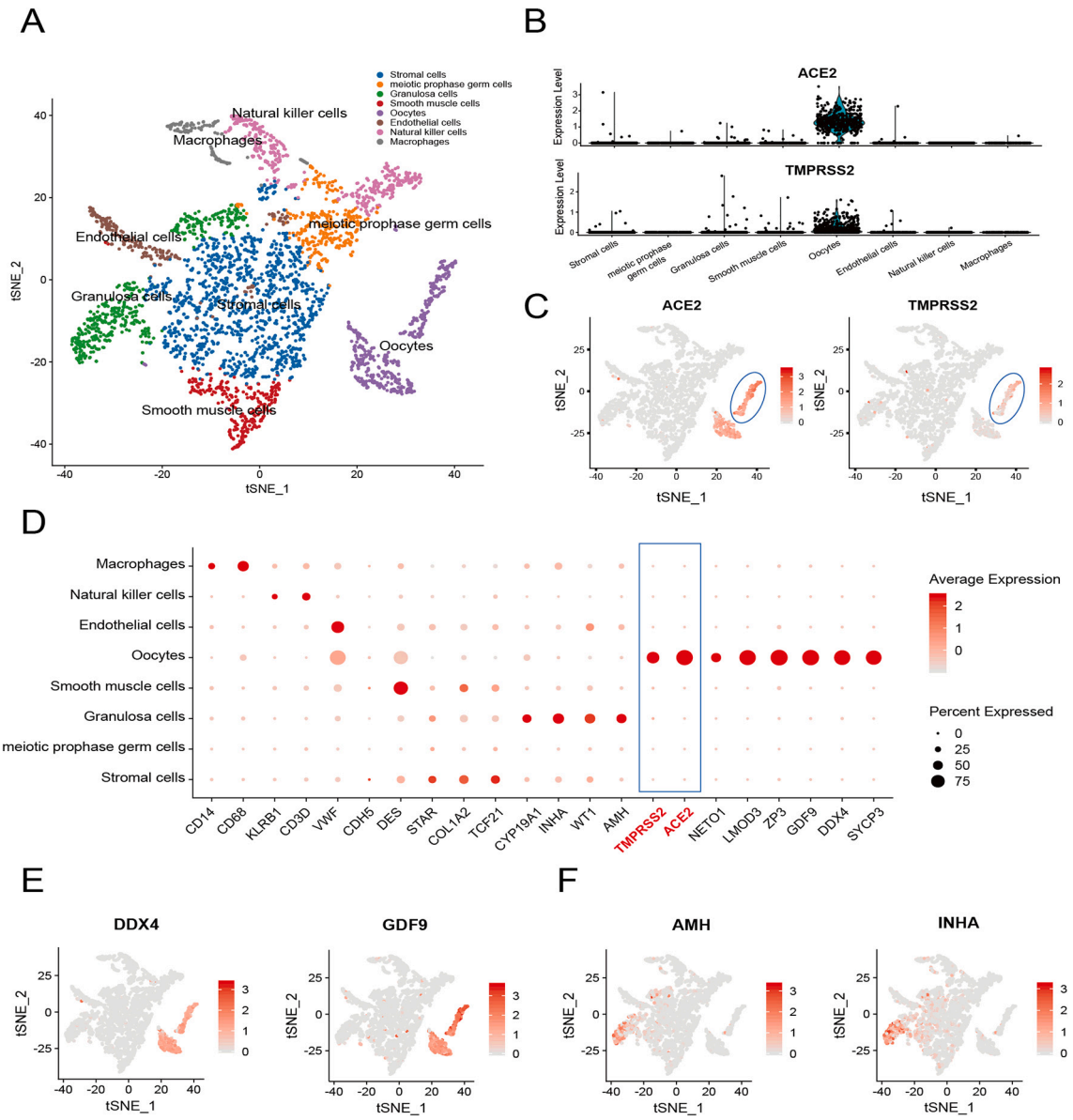

Fig. 2. Gene expression profiles of distinct ovarian cell subpopulations based on ovarian scRNA-Seq data from dataset GSE130664 (macaque ovarian single cells).
(A) T-distributed stochastic neighbor embedding (t-SNE) clustering of adult ovarian cells into eight clusters based on the scaled data.
(B) Average expression level of *ACE2* (upper) and *TMPRSS2* (lower) in each cell cluster. The vertical coordinates represent the log-transformed [*log* (x + 1)] relative expression level of *ACE2* and *TMPRSS2*.
(C) Scatter plot of *ACE2* and *TMPRSS2* gene expression of each cell cluster. The ellipse indicates the cell cluster of oocytes that co-expressed *ACE2* and *TMPRSS2*. The number and gradient color of the legend bars show the log-transformed values of gene expression matrix raw data of each cell cluster.
(D) Dot plot of the well-known markers including *ACE2* and *TMPRSS2* in each cell cluster. The color of the legend bar of average expression reflects the mean expression. The size of the dots corresponds to the percentage of cells expressing the listed genes in each cell cluster.
(E) Scatter plots of cell clusters with canonical markers of oocytes and (F) granulosa cells.

phosphate-buffered saline (PBS) buffer and incubated with Rabbit-anti-ACE2 antibody (1:200, Proteintech, China) / TMPRSS2 (1:100, ABclonal, China) at 4 °C overnight. Subsequently, the slides were washed three times and incubated with horseradish peroxidase streptavidin solution (ZB-2404; ZSGB-Bio, Beijing, China). The positive signals were colored using DAB chromogenic agent (AR1022, Boster, Wuhan, China) and counterstained using hematoxylin. Negative controls were carried out by omitting the primary antibody.

2.5. Immunofluorescence

Ovarian tissues from humans aged 25–30 yr were formalin-fixed and paraffin-embedded. The 5 μm thickness serial sections were processed by routine procedures. The sections were deparaffinized and rehydrated through gradient series of ethanol (100, 95, 85, 75%). Then the slides were microwaved for 15 min in citrate buffer (pH = 6.0) for antigen retrieval. After cooling at room temperature, slides were blocked with 5% BSA without washing in phosphate-buffered saline (PBS) buffer and incubated with Rabbit-anti-ACE2 antibody (1:50, Proteintech, China) / Mouse-anti-TMPRSS2 (1:100, Santa Cruz Biotechnology, USA) at 4 °C overnight. Afterwards, the slides were washed three times and incubated with Fitc-conjugated Donkey Anti-Rabbit / Cy3-conjugated Donkey Anti-mouse (Servicebio, China). Then, sections were washed three times in PBS and mounted with Hoechst (Servicebio, China). Images were captured using an Axio Imager upright microscope with fluorescence microscope (Olympus, Germany). Negative controls were carried out by

Table 2
The distribution of ACE2 and TMPRSS2 in each type of ovarian cells in two scRNA-seq.

	ACE2		TMPRSS2	
	GSE130664 (%)	GSE107746 (%)	GSE130664 (%)	GSE107746 (%)
Oocytes	95.58	86.42	68.81	16.05
Granulosa cells	2.55	67.14	3.19	10.00
meiotic prophase germ cells	0.31	–	0.00	–
Stromal cells	0.58	–	0.58	–
Smooth muscle cells	2.84	–	4.26	–
Endothelial cells	2.33	–	2.33	–
Macrophages	0.70	–	0.00	–
Natural killer cells	0.00	–	0.24	–

omitting the primary antibody.

3. Results

3.1. Profiling mRNA expression of different target proteins of SARS-CoV-2 in M. fascicularis and human ovaries

We first searched the online datasets of the GTEx project and then analyzed the expression level of *ACE2* and *TMPRSS2* in ovary. As lung is known to be the main target of SARS-CoV-2, we compared the *ACE2* and *TMPRSS2* expression between lung and ovary; there was no significant difference in the mRNA levels of *ACE2* and *TMPRSS2* between the ovaries and lungs (Fig. 1A, B). We accessed the scRNA-Seq data for macaque ovaries and human follicles in the GEO database (Table 1) to further investigate the cell type-specific expression of *ACE2* and *TMPRSS2*. As *M. fascicularis* and humans share similar genetic and physiological features [24], the results could also be suggestive. In GSE130664, eight clusters of cells in ovaries of *M. fascicularis* were observed (Fig. 2A). Overall, approximately 13.31% of all 2601 cells expressed *ACE2*; the highest proportion of these cells were oocytes (95.58%), and other cell types represented relatively lower proportions (Table 2). However, the expression profile of *TMPRSS2* indicated that 10.02% of all cell types expressed TMPRSS2, including 68.81% oocytes and other cell types (Table 2). The violin plot (Fig. 2B), feature plot (Fig. 2C) and dot plot (Fig. 2D) further demonstrated that *ACE2* and *TMPRSS2* were mainly expressed in oocytes. The cluster of oocytes was confirmed by the co-expression of *DDX4* and *GDF9* (Fig. 2E), the canonical markers of oocytes, indicating a similar pattern as *ACE2*. Another important cell in the ovary, granulosa cells with the marker of AMH and INHA (Fig. 2F), but did not express the *ACE2* and *TMPRSS2* (Fig. 2D). Similarly, the expression of *ACE2* and *TMPRSS2* was observed to be extremely low in the subset of macrophages and natural killer (NK) cells (Fig. 2D).

Next, we downloaded transcriptomic sequencing data for human ovary follicles (GSE107746) and divided 151 single cells into two subclusters according to the canonical markers of oocytes and granulosa cells (Fig. 3A). We found *ACE2* expression in most oocytes (86.42%) and expression in some granulosa cells (67.14%) (Fig. 3B-D, Table 2). Moreover, *ACE2* was highly expressed in some oocytes, which is similar to the expression of oocyte markers such as *DDX4* and *DAZL* (Fig. 3E) Low expression of ACE2 was observed in human ovarian granulosa cells with the marker of STAR and AMH (Fig. 3).However, 16.05% of all oocytes and 10.00% of granulosa cells were estimated to express *TMPRSS2*, showing a significantly lower expression rate than *ACE2* (Fig. 3D).

In addition, we analyzed the expression profile of two other potential SARS-CoV-2 infection-related genes, *BSG* and *CTSL* (Fig. S1). In GSE130664, *BSG* was mainly expressed in granulosa cells; However, *CTSL* was undetectable (Fig. S1—B). In GSE107764, both *BSG* and *CTSL* were mainly expressed in parts of the granulosa cells (Fig. S1—D). Together, our analysis of the public datasets indicates that SARS-CoV-2 receptor proteins are expressed in *M. fascicularis* and human ovaries, especially in oocytes and partial granulosa cells.

3.2. No observed variation in both ACE2 and TMPRSS2 expression in ovaries of different ages

To further explore the difference in *ACE2* and *TMPRSS2* gene expression between ovaries of different ages, we compared ovarian single cells from old (18–20 yr) and young (4–5 yr) *M. fascicularis* (corresponding to human females aged ~70 yr and young ovaries ~20 yr, respectively) from dataset GSE130664; human ovarian cumulus cells of old (>40 yr) and young (<35 yr) females from dataset GSE81579; and selected data on human ovarian tissues of different ages (20–79 yr) retrieved from GTEx.

Dividing each cell cluster into old and young groups showed that the percentage expression levels (Fig. 4A) and average expression levels of *ACE2* and *TMPRSS2* did not significantly differ between old and young ovarian cells (Fig. 4C). Fig. 4B presents the visual outliers on a scatter plot with the significant DEGs displayed in an ellipse; however, *ACE2* and *TMPRSS2* expression were not included. Although *ACE2* was identified as a DEG in the oocyte cluster, the average logFC value was 0.321, and the adjusted *P*-value was 1, indicating non-significant differential expression. The DEGs of other clusters between old and young groups did not include *ACE2* or *TMPRSS2*. The specific values of differential expression analysis are listed in Table 3.

Moreover, we explored bulk RNA-Seq data of old and young human ovaries retrieved from the GEO and GTEx databases. The upregulated and downregulated gene expression patterns in dataset GSE81579 demonstrated that *ACE2* was not included in the DEGs of cumulus cells between young and old females (Fig. 4D). The data of human ovarian tissue from GTEx was also analyzed; both *ACE2* and *TMPRSS2* were not differentially expressed during ovarian aging (Fig. 4E). In addition, the analysis of dataset GSE87201 revealed that both *ACE2* and *TMPRSS2* were not differentially expressed in oocytes between low and high ovarian reserve (Fig. 4F). From the results mentioned above, we concluded that there was no disparity in *ACE2* or *TMPRSS2* expression between ovaries of different ages or with different ovarian reserve conditions in all available datasets. The specific description of each dataset is listed in Table 1.

3.3. ACE2 and TMPRSS2 protein co-expression in human ovaries from puberty to menopause

Next, we validated the results of transcriptome analysis by using immunohistochemistry in human ovaries. Immunoreactivity for ACE2 was found to be distributed in multiple regions of human ovary. As shown in Fig. 5A, ACE2 was highly expressed in the ovarian cortex from sexual maturity to menopause, especially in oocytes and stromal cells. In addition, immunohistochemistry of human ovaries from 14 to 60 yr-old individuals revealed that TMPRSS2 was also expressed in the ovarian cortex of all ages, especially in oocytes (Fig. 5B). We found no difference in the expression of TMPRSS2 in ovaries of different ages, which was consistent with the results of RNA sequencing analysis. To confirm the specificity of the antibodies against ACE2 and TMPRSS2, we performed negative controls with PBS, and used testis sections in positive controls since were reported to overexpress ACE2.

Next, we explored the expression of ACE2 and TMPRSS2 in human ovarian medulla of different ages. The results showed that ACE2 was highly expressed in the ovarian medulla from sexual maturity to menopause but not during puberty (Fig. S2). Approximately 80% of the

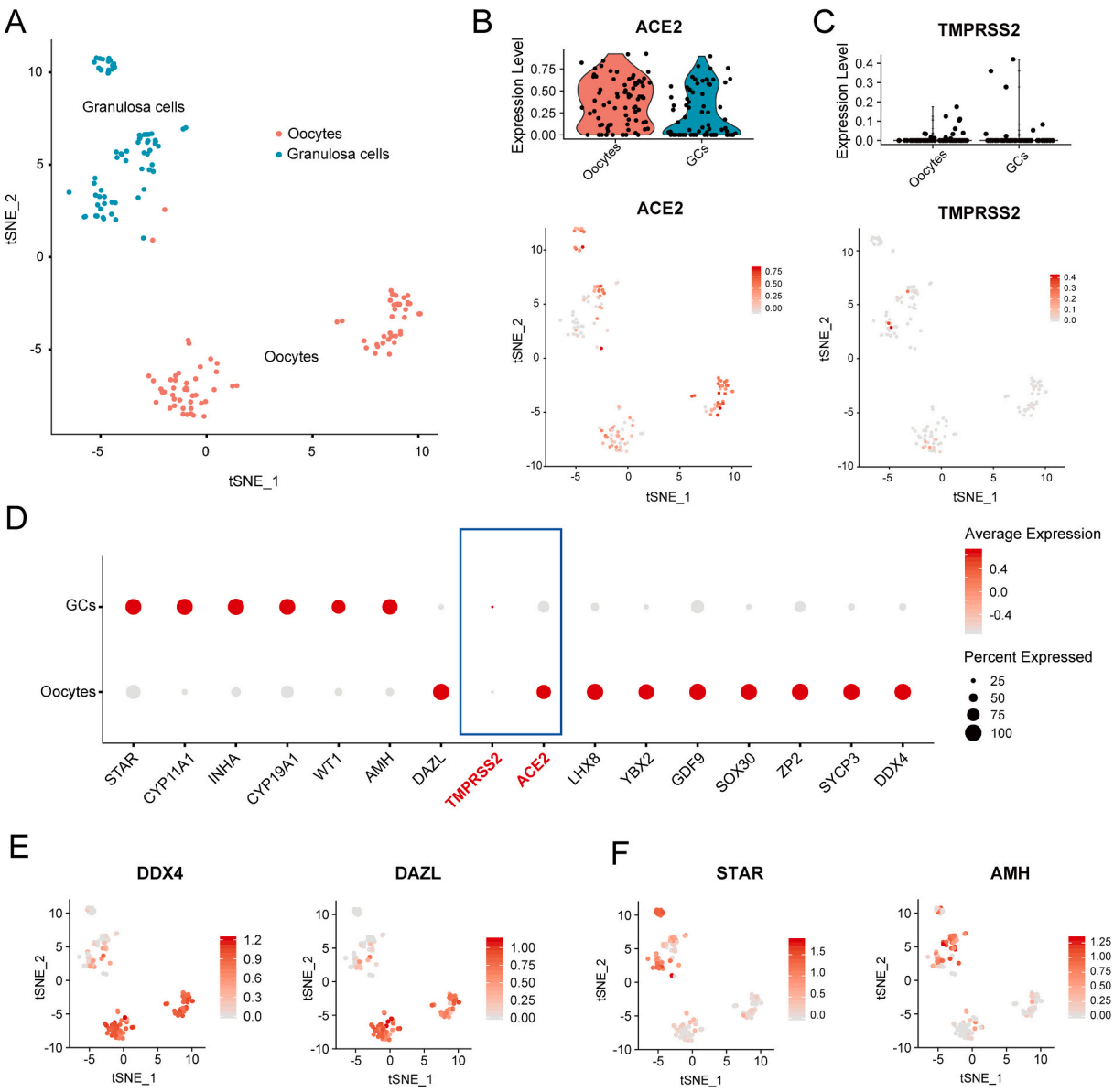

Fig. 3. Gene expression profiles of oocytes and granulosa cells based on the ovarian scRNA-Seq data from dataset GSE107746 (human oocytes and granulosa cells).
(A) T-distributed stochastic neighbor embedding (t-SNE) clustering of adult ovarian cells into two clusters—oocytes and granulosa cells.
(B) Average expression level of *ACE2* (upper) and scatter plot of *ACE2* expression (lower) in each cell cluster based on the canonical cell markers of oocytes and granulosa cells. GCs: granulosa cells. The number and gradient color of the legend bars showed the log-transformed values of gene expression matrix raw data of each cell cluster.
(C) Average expression level of *TMPRSS2* (upper) and the scatter plot of *TMPRSS2* expression (lower) of each cell cluster.
(D) Dot plot of the well-known markers including *ACE2* and *TMPRSS2* in each cell cluster. The color of the legend bar of average expression reflects the mean expression. The size of the dots corresponds to the percentage of cells expressing the listed genes in each cell cluster.
(E) Scatter plots of cell clusters with the markers of oocytes and (F) granulosa cells.

ovarian medullary cells were positive for ACE2. Blood vessels and matrix cells showed intense immunoreactivity for ACE2 (Fig. S2A). The immunoreactivity data suggested that TMPRSS2 was highly expressed in human ovarian medullary blood vessels and stromal cells (Fig. S2B). In conclusion, ACE2 and TMPRSS2 are expressed in human ovarian medulla.

As ovarian follicles play an essential role in ovarian function, we further explored the expression of ACE2 and TMPRSS2 in ovarian follicles of different stages. As shown in Fig. 6, ACE2 (Fig. 6A) and TMPRSS2 (Fig. 6B) immunoreactivity was observed in all phases of follicle development. In primordial follicles, intense ACE2 and TMPRSS2 immunostaining appeared in the oocytes. Strong immunoreactivity for ACE2 and TMPRSS2 was also observed both in oocytes and the granulosa layer of primary follicles. In secondary follicles, the granulosa cells were negative for ACE2, whereas the theca-interstitial cells showed moderate staining for ACE2, and TMPRSS2 was highly expressed in some granulosa cells. In antral follicles, ACE2 was highly expressed in the outer granulosa cells, but the inner granulosa cells were moderate staining. Expression of TMPRSS2 was clearly localized in some granulosa cells and theca-interstitial cells. The cytoplasm of small and large luteal cells in corpora lutea showed intense staining for ACE2 and TMPRSS2. Taken together, ACE2 and TMPRSS2 were expressed in all stages of the follicles, which was consistent with the results of the RNA-Seq analysis.

Furthermore, a double immunofluorescence study was performed to explore the relationship between ACE2 and TMPRSS2 expression. The

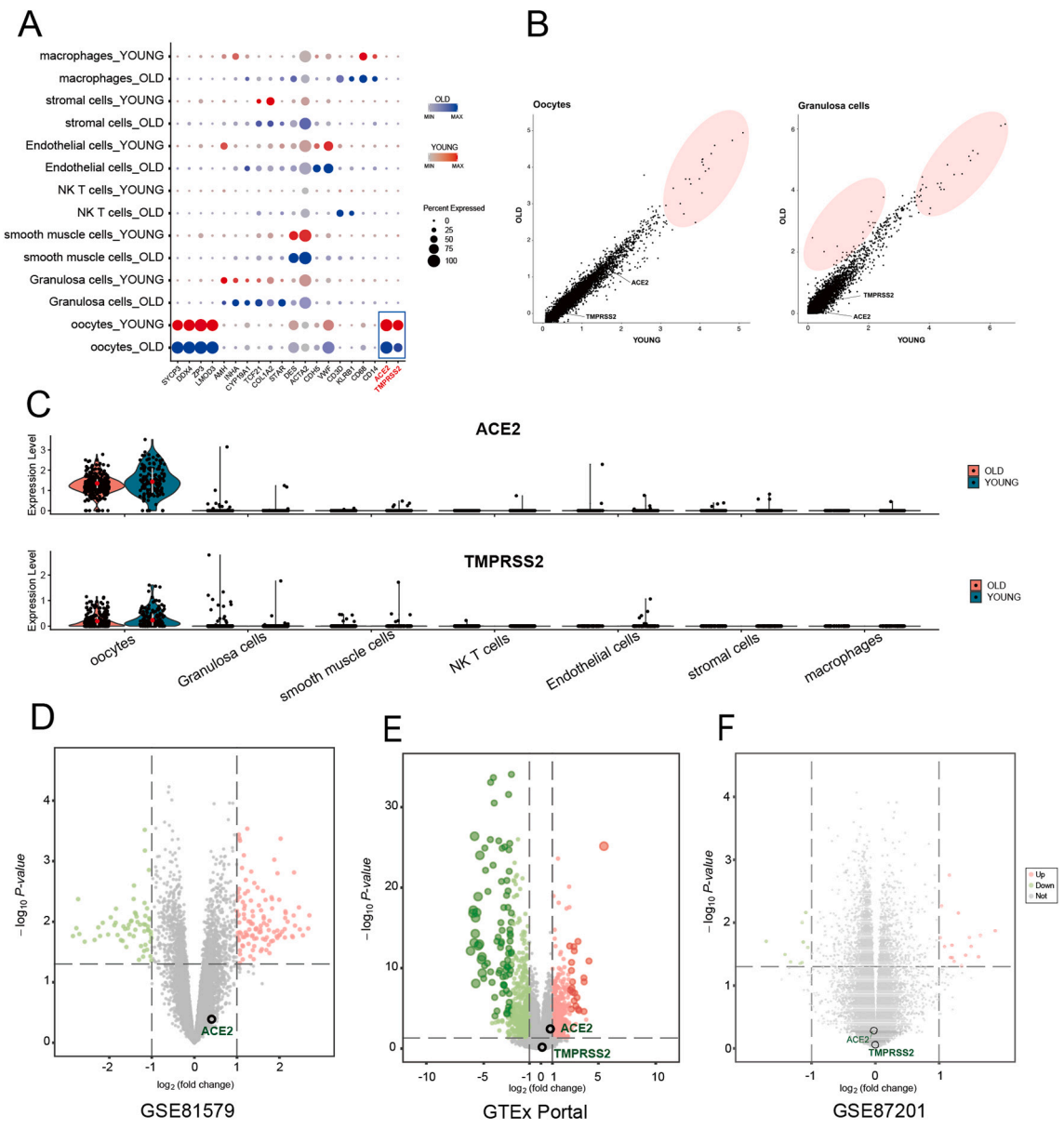

Fig. 4. *ACE2* or *TMPRSS2* gene expression did not significantly differ between old and young ovaries.
(A) Dot plot of each cell cluster in GSE130664 (macaque ovarian single cells) in old and young groups, showing the expression level and percentage of cells in a cluster expressing conserved markers (including *ACE2* and *TMPRSS2*).
(B) Comparative analysis of oocytes and granulosa cells in GSE130664 (macaque ovarian single cells) to visualize *ACE2* and *TMPRSS2* expression with the outlier scatter plot. The ellipse indicates the differentially expressed genes between old and young ovarian single cells.
(C) Violin plots show the expression level and distribution of *ACE2* and *TMPRSS2* in all ovarian single cells from all seven cell types of each ovarian cell cluster in old and young groups in GSE130664 (macaque ovarian single cells). The vertical coordinates represent the log-transformed [*log* (x + 1)] relative expression level of *ACE2*. The average expression level of *ACE2* and *TMPRSS2* showed no significant differences between old and young ovarian single cells.
(D) Volcano plot of aged and young human cumulus cells in dataset GSE81579 (bulk RNA-Seq of human cumulus cells), with ACE2 (black circle) included among the genes that showed non-significant differential expression (grey circles); however, TMPRSS2 was not detected.
(E) Volcano plot of bulk RNA-Seq of aged and young ovarian tissues in Genotype-Tissue Expression (GTEx) project (bulk RNA-Seq of human ovarian tissues); neither *ACE2* nor *TMPRSS2* (black circles) was differentially expressed.
(F) Volcano plot of oocytes with low and high ovarian reserve in dataset GSE87201 (bulk RNA-Seq of human oocytes), neither *ACE2* nor *TMPRSS2* (black circles) was differentially expressed.

results suggested co-expression of ACE2 and TMPRSS2 in the ovarian cortex, medulla, and follicles (Fig. 7, Fig. S3). Together, these results suggest the co-expression of ACE2 and TMPRSS2 in human ovaries.

3.4. *Virus-related potential biological processes in ACE2/TMPRSS2-positive macaque ovarian cells*

We compared the features of ACE2/TMPRSS2-positive and ACE2/TMPRSS2-negative ovarian cells in dataset GSE130064 (macaque ovarian single cells) through a DEG functional analysis. The GO functional enrichment analysis indicated that eight virus-related biological process terms were enriched in ACE2-positive oocytes/granulosa cells, including viral transcription, viral gene expression, viral entry into host cells and viral life cycle (Fig. 8A, Table S2). The specific genes enriched in the GO terms were visualized in a heatmap-like functional plot (Fig. 8C), mainly focusing on the L ribosomal protein family. KEGG

Table 3
The expression status of ACE2 and TMPRSS2 between old and young oocytes/granulosa cells.

Gene	Cell type	Average expression value	Percentage of expression (%)	Scaled average expression
TMPRSS2	Old granulosa cells	0.029124	1.536984	4
TMPRSS2	Young granulosa cells	0.014594	1.526718	3
TMPRSS2	Old oocytes	0.250906	64.78405	14
TMPRSS2	Young oocytes	0.473481	81.11888	20
ACE2	Old granulosa cells	0.025505	1.056676	3
ACE2	Young granulosa cells	0.012305	1.272265	3
ACE2	Old oocytes	3.003148	97.00997	16
ACE2	Young oocytes	4.520156	95.8042	20

pathway analysis showed that a series of viral infection pathways (human papillomavirus infection, human T-cell leukemia virus 1 infection, human cytomegalovirus infection, and viral carcinogenesis) were enriched in ACE2-positive ovarian cells (Fig. 8B). Moreover, the focal adhesion pathway may be engaged in regulating virus entry and host response. Furthermore, the functional enrichment analysis of TMPRSS2-positive and TMPRSS2-negative ovarian cells showed that the enriched pathways were mainly involved in the female reproductive process, including oogenesis and oocyte development (Fig. 8D, Table S3). The significant KEGG pathways were enriched in oocyte meiosis, homologous recombination, and mismatch repair pathway, indicating the underlying affected meiotic prophase biological events (Fig. 8E). On the basis of the above analysis, we speculate that SARS-CoV-2 may potentially target ACE-positive ovarian cells and therefore influence oogenesis; however, this speculation still lacks direct evidence.

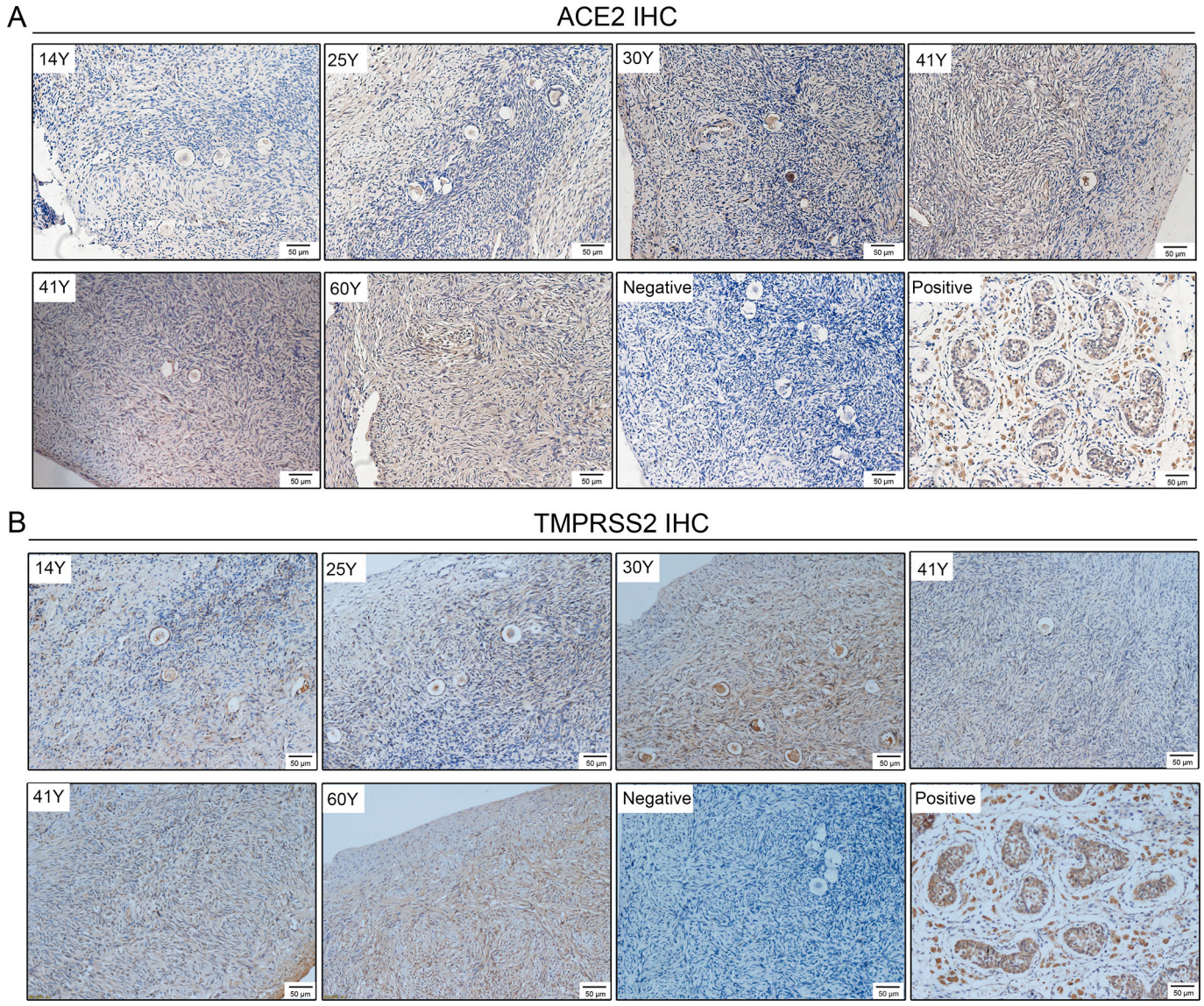

Fig. 5. Representative images of ACE2 (A) and TMPRSS2 (B) immunohistochemical staining in the human ovarian cortex of different ages (14 to 60 yr). The positive control was human testis. The negative control was carried out by omitting the primary antibody.

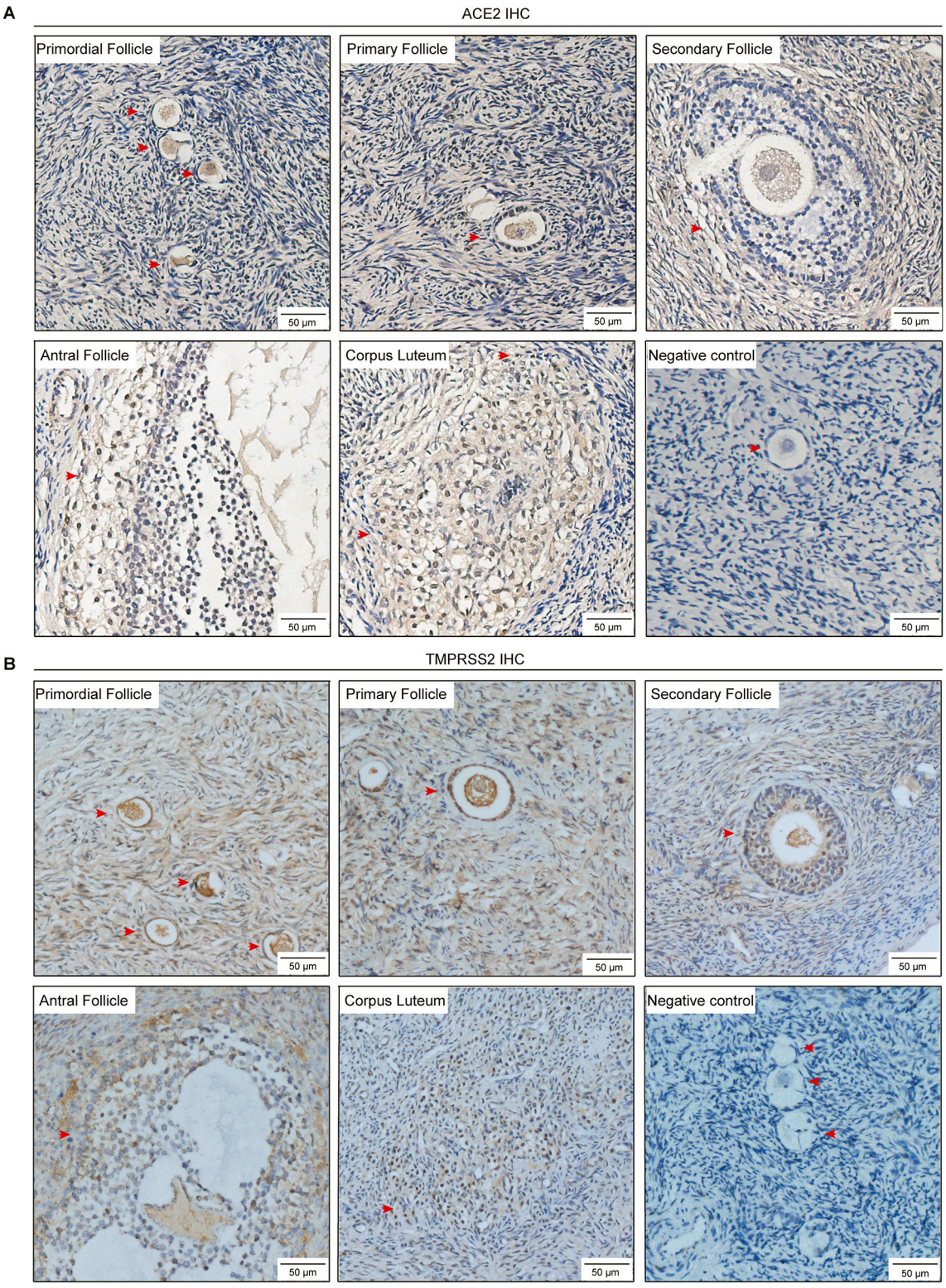

Fig. 6. Immunohistochemical staining indicated that the expression of ACE2 (A) and TMPRSS2 (B) occurred in all types of human follicles. The red arrows indicate follicles. The negative control was carried out by omitting the primary antibody. (For interpretation of the references to color in this figure legend, the reader is referred to the web version of this article.)

4. Discussion

The ongoing 2019–2020 COVID-19 pandemic has become a severe public health problem worldwide. As the COVID-19 pandemic continues, the health of more and more young women is threatened. The maintenance of the ovarian reproductive and endocrine function in females is related to the health of the individual and the next generation. Therefore, the crucial question that needs to be addressed is whether the SARS-CoV-2 infection would cause ovarian dysfunction. Recently, the pathological results from the systematic autopsy of COVID-19 victims in

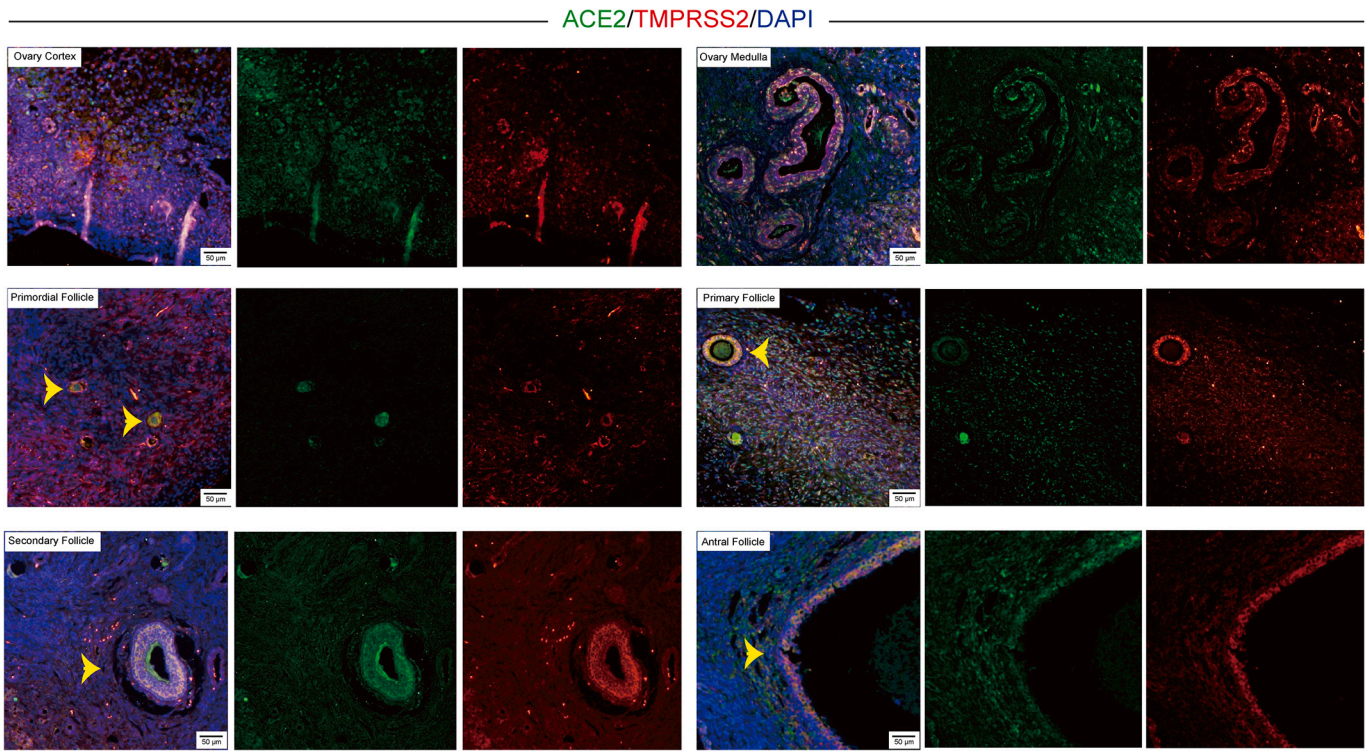

Fig. 7. Immunofluorescence staining showed the co-expression of ACE2 and TMPRSS2 in human ovaries. The yellow arrows indicate follicles. The blue channel is DAPI staining, the green channel is ACE2 expression, and the red channel is TMPRSS2 expression. (For interpretation of the references to color in this figure legend, the reader is referred to the web version of this article.)

China demonstrated the presence of RNA and viral particles of SARS-CoV-2 in the ovary through PCR, transmission electron microscopy, and immunohistochemical staining [12]. However, it remains unclear how SARS-CoV-2 infects the ovary. In the present study, on the basis of scRNA-Seq data of human and non-human primate ovary and immunohistochemical experiments, we identified the co-expression of the two key entry molecules for SARS-CoV-2, ACE2 and TMPRSS2, in oocytes, luteal cells, blood vessels, and some matrix cells in human ovaries of different ages.

Several types of viruses are reported to directly infect the ovary and cause decreased ovarian function, such as endogenous retroviruses (found in the human ovary) and human immunodeficiency virus (HIV; in human germ cells) [25,26]. In addition, hepatitis B virus, herpes simplex virus, and adenoviruses can also be detected in ovarian tissue, including oocytes, granulosa cells and other cells [27–29]. The mumps virus and HIV are the most recognized and extensively studied viruses that can potentially cause ovarian damage in humans. A multicenter study by Cejtin et al. [26] including 1139 HIV-seropositive and 292 HIV-seronegative women indicated that HIV-positive women were three times more likely to have protracted amenorrhea than HIV-negative women (10.5% vs. 5.5%). Moreover, the fertility of HIV-seropositive women who do not receive antiretroviral treatment may be lower than that of the seronegative control group [30,31]. Nonetheless, it remains unclear whether SARS-CoV-2 infection results in declined ovarian function. Another point of concern is whether the fertility of SARS-CoV-2-infected women will be adversely affected. While Rotshenker-Olshinka et al. reported that the COVID-19 infection did not seem to affect early first-trimester miscarriage rates in asymptomatic patients [32][], but there is still a lack of rigorous randomized controlled clinical studies. Therefore, clinicians should pay attention to ovarian function in female patients with SARS-CoV-2 infection.

The major changes in the ovary due to viral infections include germ cell apoptosis, interstitial inflammation, leukocyte infiltration, and fibrosis [33]. Pathological studies have identified that SARS-CoV-2 infection lead to interstitial edema; monocyte, lymphocyte, and neutrophil infiltration; tunica intima inflammation, and cell degeneration in multiple organs [12]. In addition, some studies suggest that the severity and prognosis of COVID-19 is related to an excessive production of the pro-inflammatory cytokine cascades, also known as a cytokine storm [34]. Patients with COVID-19 with varying disease severity (mild to severe) had different levels of various cytokines and chemokines. Preliminary research indicates that plasma levels of interleukin (IL)-1β, IL-1RA, IL-7, IL-8, IL-10, IFN-γ, monocyte chemoattractant peptide-1, macrophage inflammatory protein (MIP)-1A, MIP-1B, granulocyte colony-stimulating factor, and tumor necrosis factor-alpha (TNF-α) were elevated in patients with COVID-19 [35]. Moreover, the plasma levels of IL-2, IL-6, IL-8, IL-10, and TNF-α were significantly higher in patients with severe infection than in those with non-severe infections [36]. A significant number of domestic and foreign studies have confirmed that inflammation mediates changes in the follicular function, which weakens the ability of oocytes to complete meiosis and undergo fertilization and embryo development up to the blastocyst stage and beyond [37–39]. Oocytes and ovarian cells are also susceptible to oxidative damage, which may deplete the ovarian reserve of primordial follicles and damage the surviving oocytes sufficiently to render them incapable of fertilization or normal development after fertilization; it follows that inflammatory factors may be a vital cause of POI [40]. Therefore, SARS-CoV-2 infection may affect ovarian function by directly binding to the ACE2 or TMPRSS2 receptor or indirectly through the cytokine storm.

In conclusion, we demonstrated the co-expression of the SARS-CoV-2 receptors ACE2 and TMPRSS2 in human ovaries. Therefore, when evaluating the prognosis of COVID-19, ovarian damage and offspring health should be given significant attention. However, further clinical and fundamental research is still needed to monitor the long-term effects of the SARS-CoV-2 on the reproductive system in recovered female patients.

Supplementary data to this article can be found online at https://doi.org/10.1016/j.ygeno.2021.08.012.

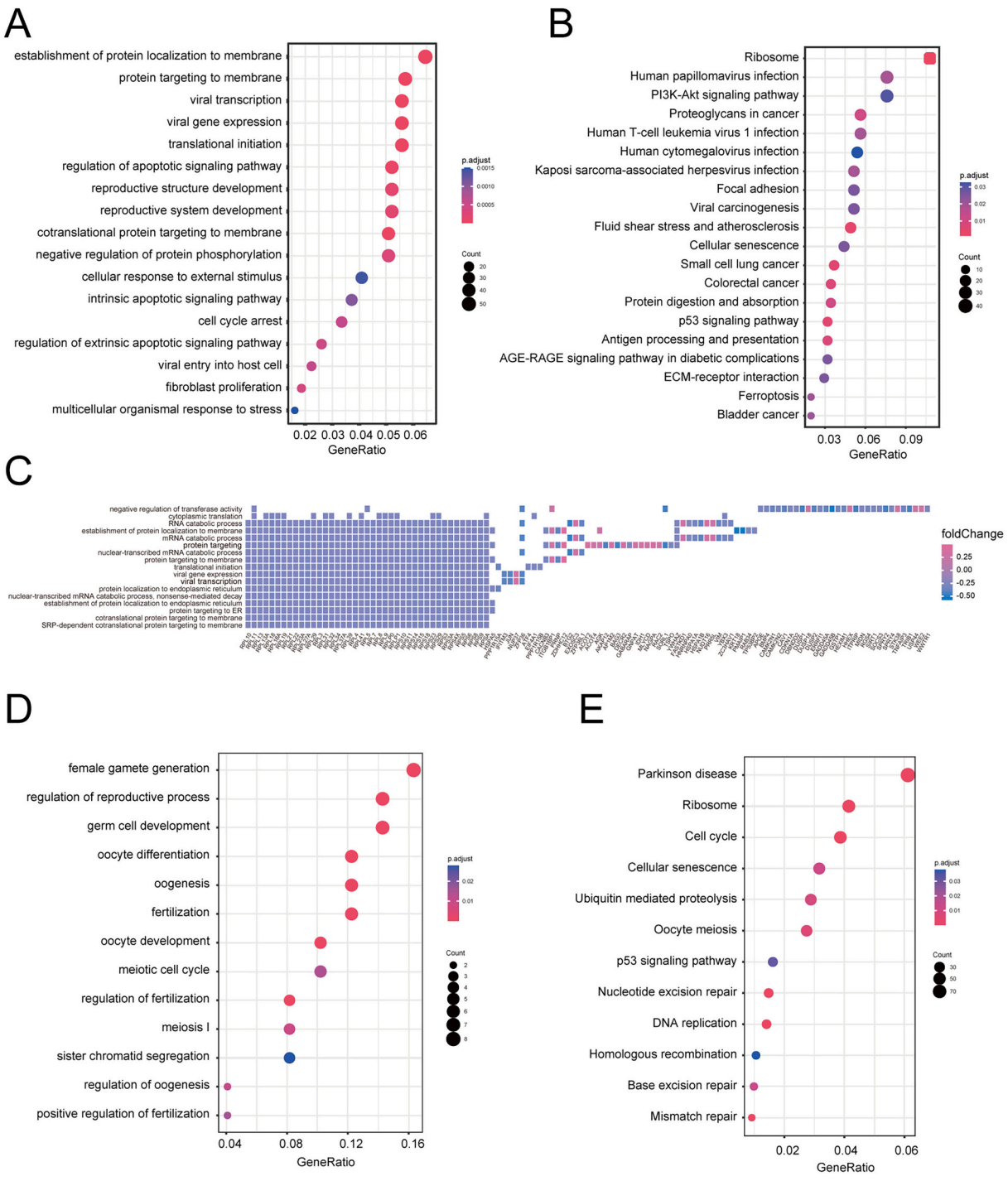

Fig. 8. Differentially expressed gene (DEG) functional analysis of *ACE2* and *TMPRSS2* in macaque single ovarian cells (GSE130664).
(A) Gene ontology (GO) enrichment results (only biological process terms shown) of DEGs in ACE2-positive and ACE2-negative ovarian cells.
(B) Kyoto Encyclopedia of Genes and Genomes (KEGG) pathway enrichment analysis of DEGs in *ACE2*-positive and *ACE2*-negative ovarian cells.
(C) Visualization of the relationships of GO terms and corresponding mapped genes.
(D) GO enrichment result (only BP terms shown) of DEGs in *TMPRSS2*-positive and *TMPRSS2*-negative ovarian cells.
(E) KEGG pathway enrichment analysis of DEGs in *TMPRSS2*-positive and *TMPRSS2*-negative ovarian cells. BP: biological process.

Authors' contribution

M.W., L.M., J.Z. and S.W. conceived and coordinated the study; M.W. and L.M. conducted all the major experiments and wrote the manuscript; L.X., S.Z., J.D. and W.Y. performed and analyzed the experiments; Q.Z. collected human ovarian tissues.

Funding

This work was supported by grants from the National Natural Science Foundation of China (No. 82001514, 81671394 and 81873824) and the Clinical Research Pilot Project of Tongji Hospital, Huazhong University of Science and Technology (No. 2019CR205).

Declaration of Competing Interest

The authors declare that they have no conflict of interest.

Acknowledgements

We thank all the patients who took part in our study. Technical support with figures and drafting from Chris_Life_Science (Blogger, WeChat Official Accounts) is gratefully acknowledged.

References

[1] J.F.-W. Chan, S. Yuan, K.-H. Kok, K.K.-W. To, H. Chu, J. Yang, F. Xing, J. Liu, C.C.-Y. Yip, R.W.-S. Poon, H.-W. Tsoi, S.K.-F. Lo, K.-H. Chan, V.K.-M. Poon, W.-M. Chan, J.D. Ip, J.-P. Cai, V.C.-C. Cheng, H. Chen, C.K.-M. Hui, K.-Y. Yuen, A familial cluster of pneumonia associated with the 2019 novel coronavirus indicating person-to-person transmission: a study of a family cluster, Lancet 395 (2020) 514–523.

[2] P. Zhou, X.-L. Yang, X.-G. Wang, B. Hu, L. Zhang, W. Zhang, H.-R. Si, Y. Zhu, B. Li, C.-L. Huang, H.-D. Chen, J. Chen, Y. Luo, H. Guo, R.-D. Jiang, M.-Q. Liu, Y. Chen, X.-R. Shen, X. Wang, X.-S. Zheng, K. Zhao, Q.-J. Chen, F. Deng, L.-L. Liu, B. Yan, F.-X. Zhan, Y.-Y. Wang, G.-F. Xiao, Z.-L. Shi, A pneumonia outbreak associated with a new coronavirus of probable bat origin, Nature 579 (2020) 270–273.

[3] W. Li, M.J. Moore, N. Vasilieva, J. Sui, S.K. Wong, M.A. Berne, M. Somasundaran, J.L. Sullivan, K. Luzuriaga, T.C. Greenough, H. Choe, M. Farzan, Angiotensin-converting enzyme 2 is a functional receptor for the SARS coronavirus, Nature 426 (2003) 450–454.

[4] M. Hoffmann, H. Kleine-Weber, S. Schroeder, N. Krüger, T. Herrler, S. Erichsen, T. S. Schiergens, G. Herrler, N.-H. Wu, A. Nitsche, M.A. Müller, C. Drosten, S. Pöhlmann, SARS-CoV-2 Cell Entry Depends on ACE2 and TMPRSS2 and Is Blocked by a Clinically Proven Protease Inhibitor, Cell 181 (2020).

[5] S. Matsuyama, N. Nao, K. Shirato, M. Kawase, S. Saito, I. Takayama, N. Nagata, T. Sekizuka, H. Katoh, F. Kato, M. Sakata, M. Tahara, S. Kutsuna, N. Ohmagari, M. Kuroda, T. Suzuki, T. Kageyama, M. Takeda, Enhanced isolation of SARS-CoV-2 by TMPRSS2-expressing cells, Proc. Natl. Acad. Sci. U. S. A. 117 (2020) 7001–7003.

[6] R. Zang, M.F. Gomez Castro, B.T. McCune, Q. Zeng, P.W. Rothlauf, N.M. Sonnek, Z. Liu, K.F. Brulois, X. Wang, H.B. Greenberg, M.S. Diamond, M.A. Ciorba, S.P. J. Whelan, S. Ding, TMPRSS2 and TMPRSS4 promote SARS-CoV-2 infection of human small intestinal enterocytes, Sci Immunol 5 (2020).

[7] D. Harmer, M. Gilbert, R. Borman, K.L. Clark, Quantitative mRNA expression profiling of ACE 2, a novel homologue of angiotensin converting enzyme, FEBS Lett. 532 (2002) 107–110.

[8] I. Hamming, W. Timens, M.L.C. Bulthuis, A.T. Lely, G.J. Navis, H. van Goor, Tissue distribution of ACE2 protein, the functional receptor for SARS coronavirus. A first step in understanding SARS pathogenesis, J Pathol 203 (2004) 631–637.

[9] S.A. Lauer, K.H. Grantz, Q. Bi, F.K. Jones, Q. Zheng, H.R. Meredith, A.S. Azman, N. G. Reich, J. Lessler, The incubation period of coronavirus disease 2019 (COVID-19) from publicly reported confirmed cases: estimation and application, Ann. Intern. Med. 172 (2020) 577–582.

[10] M. Gheblawi, K. Wang, A. Viveiros, Q. Nguyen, J.-C. Zhong, A.J. Turner, M. K. Raizada, M.B. Grant, G.Y. Oudit, Angiotensin-converting enzyme 2: SARS-CoV-2 receptor and regulator of the renin-angiotensin system: celebrating the 20th anniversary of the discovery of ACE2, Circ. Res. 126 (2020) 1456–1474.

[11] B. Xu, M.U.G. Kraemer, Open access epidemiological data from the COVID-19 outbreak, Lancet Infect. Dis. 20 (2020) 534.

[12] X.-W. Bian, C.-P.T, Autopsy of COVID-19 victims in China, Natl Sci Rev (2020) nwaa123.

[13] Z. Wang, X. Xu, scRNA-seq Profiling of Human Testes Reveals the Presence of the ACE2 Receptor, A Target for SARS-CoV-2 Infection in Spermatogonia, Leydig and Sertoli Cells, Cells 9 (2020).

[14] J. Goad, J. Rudolph, A. Rajkovic, Female reproductive tract has low concentration of SARS-CoV2 receptors, Plos One 15 (2020) e0243959, the preprint server for biology.

[15] K.E. Stanley, E. Thomas, M. Leaver, D. Wells, Coronavirus disease-19 and fertility: viral host entry protein expression in male and female reproductive tissues, Fertil. Steril. 114 (2020) 33–43.

[16] M. Prajapat, P. Sarma, N. Shekhar, A. Prakash, P. Avti, A. Bhattacharyya, H. Kaur, S. Kumar, S. Bansal, A.R. Sharma, B. Medhi, Update on the target structures of SARS-CoV-2: a systematic review, Indian J Pharmacol 52 (2020) 142–149.

[17] A. Battle, C.D. Brown, B.E. Engelhardt, S.B. Montgomery, Genetic effects on gene expression across human tissues, Nature 550 (2017) 204–213.

[18] Human Genomics, The Genotype-Tissue Expression (GTEx) pilot analysis: multitissue gene regulation in humans, Science 348 (2015) 648–660.

[19] T. Stuart, A. Butler, P. Hoffman, C. Hafemeister, E. Papalexi, W.M. Mauck, Y. Hao, M. Stoeckius, P. Smibert, R. Satija, Comprehensive integration of single-cell data, Cell 177 (2019).

[20] S. Wang, Y. Zheng, J. Li, Y. Yu, W. Zhang, M. Song, Z. Liu, Z. Min, H. Hu, Y. Jing, X. He, L. Sun, L. Ma, C.R. Esteban, P. Chan, J. Qiao, Q. Zhou, J.C. Izpisua Belmonte, J. Qu, F. Tang, G.-H. Liu, Single-cell transcriptomic atlas of primate ovarian aging, Cell 180 (2020).

[21] Y. Zhang, Z. Yan, Q. Qin, V. Nisenblat, H.-M. Chang, Y. Yu, T. Wang, C. Lu, M. Yang, S. Yang, Y. Yao, X. Zhu, X. Xia, Y. Dang, Y. Ren, P. Yuan, R. Li, P. Liu, H. Guo, J. Han, H. He, K. Zhang, Y. Wang, Y. Wu, M. Li, J. Qiao, J. Yan, L. Yan, Transcriptome landscape of human folliculogenesis reveals oocyte and granulosa cell interactions, Mol Cell 72 (2018).

[22] X. Zhang, Y. Lan, J. Xu, F. Quan, E. Zhao, C. Deng, T. Luo, L. Xu, G. Liao, M. Yan, Y. Ping, F. Li, A. Shi, J. Bai, T. Zhao, X. Li, Y. Xiao, CellMarker: a manually curated resource of cell markers in human and mouse, Nucleic Acids Res. 47 (2019) D721–D728.

[23] G. Yu, L.-G. Wang, Y. Han, Q.-Y. He, clusterProfiler: an R package for comparing biological themes among gene clusters, OMICS 16 (2012) 284–287.

[24] J.D. Harding, Progress in genetics and genomics of nonhuman primates. Introduction, ILAR J. 54 (2013) 77–81.

[25] M.M. Arimi, A. Nyachieo, D.K. Langat, A.M. Abdi, J.M. Mwenda, Evidence for expression of endogenous retroviral sequences on primate reproductive tissues and detection of cross-reactive ERVS antigens in the baboon ovary: a review, East Afr. Med. J. 83 (2006) 106–112.

[26] H.E. Cejtin, A. Kalinowski, P. Bacchetti, R.N. Taylor, D.H. Watts, S. Kim, L. S. Massad, S. Preston-Martin, K. Anastos, M. Moxley, H.L. Minkoff, Effects of human immunodeficiency virus on protracted amenorrhea and ovarian dysfunction, Obstet. Gynecol. 108 (2006) 1423–1431.

[27] H. Irie, A. Kiyoshi, A.H. Koyama, A role for apoptosis induced by acute herpes simplex virus infection in mice, Int. Rev. Immunol. 23 (2004) 173–185.

[28] J.S.M. Mak, M.B.W. Leung, C.H.S. Chung, J.P.W. Chung, L.P. Cheung, T.T. Lao, T. C. Li, Presence of hepatitis B virus DNA in follicular fluid in female hepatitis B carriers and outcome of IVF/ICSI treatment: a prospective observational study, Eur. J. Obstet. Gynecol. Reprod. Biol. 239 (2019) 11–15.

[29] A.G. Abdulmedzhidova, K.V. Rog, L.É. Zavalishina, A.A. Kushch, Intrafollicular infection of mammals and human oocytes by the herpes simplex virus, Vopr. Virusol. 59 (2014) 42–46.

[30] R.H. Gray, M.J. Wawer, D. Serwadda, N. Sewankambo, C. Li, F. Wabwire-Mangen, L. Paxton, N. Kiwanuka, G. Kigozi, J. Konde-Lule, T.C. Quinn, C.A. Gaydos, D. McNairn, Population-based study of fertility in women with HIV-1 infection in Uganda, Lancet 351 (1998).

[31] V.A. Kushnir, W. Lewis, Human immunodeficiency virus/acquired immunodeficiency syndrome and infertility: emerging problems in the era of highly active antiretrovirals, Fertil. Steril. 96 (2011) 546–553.

[32] K. Rotshenker-Olshinka, A. Volodarsky-Perel, N. Steiner, E. Rubenfeld, M. H. Dahan, COVID-19 pandemic effect on early pregnancy: are miscarriage rates altered, in asymptomatic women? Arch Gynecol Obstet 303 (2020) 839–845.

[33] E.A. Caine, S.M. Scheaffer, D.E. Broughton, V. Salazar, J. Govero, S. Poddar, A. Osula, J. Halabi, M.E. Skaznik-Wikiel, M.S. Diamond, K.H. Moley, Zika virus causes acute infection and inflammation in the ovary of mice without apparent defects in fertility, J. Infect. Dis. 220 (2019) 1904–1914.

[34] F. Coperchini, L. Chiovato, L. Croce, F. Magri, M. Rotondi, The cytokine storm in COVID-19: an overview of the involvement of the chemokine/chemokine-receptor system, Cytokine Growth Factor Rev. 53 (2020) 25–32.

[35] A. Tufan, A. Avanoğlu Güler, M. Matucci-Cerinic, COVID-19, immune system response, hyperinflammation and repurposing antirheumatic drugs, Turkish journal of medical sciences 50 (2020) 620–632.

[36] C. Qin, L. Zhou, Z. Hu, S. Zhang, S. Yang, Y. Tao, C. Xie, K. Ma, K. Shang, W. Wang, D.-S. Tian, Dysregulation of immune response in patients with coronavirus 2019 (COVID-19) in Wuhan, China, Clinical Infectious Diseases 71 (2020) 762–768.

[37] M. Goldsammler, Z. Merhi, E. Buyuk, Role of hormonal and inflammatory alterations in obesity-related reproductive dysfunction at the level of the hypothalamic-pituitary-ovarian axis, Reprod. Biol. Endocrinol. 16 (2018) 45.

[38] A.K. Singh, M. Dutta, R. Chattopadhyay, B. Chakravarty, K. Chaudhury, Intrafollicular interleukin-8, interleukin-12, and adrenomedullin are the promising prognostic markers of oocyte and embryo quality in women with endometriosis, J. Assist. Reprod. Genet. 33 (2016) 1363–1372.

[39] S. Vannuccini, V.L. Clifton, I.S. Fraser, H.S. Taylor, H. Critchley, L.C. Giudice, F. Petraglia, Infertility and reproductive disorders: impact of hormonal and inflammatory mechanisms on pregnancy outcome, Hum. Reprod. Update 22 (2016) 104–115.

[40] R.O. Gilbert, Symposium review: mechanisms of disruption of fertility by infectious diseases of the reproductive tract, J. Dairy Sci. 102 (2019) 3754–3765.